IOSR Journal of Electronics and Communication Engineering (IOSR-JECE)
e-ISSN: 2278-2834,p- ISSN: 2278-8735.Volume 14, Issue 1, Ver. I (Jan.-Feb. 2019), PP 22-30
www.iosrjournals.org

The Influence of Bit Error Rate on DWDM System with Different Pumping Powers in EDFA

Petr Ivaniga[1], Slavomíra Kureková[1], Tomáš Ivaniga[2]
[1]*(Department of Transportation Networks, Faculty of Management Science and Informatics/ University of Žilina, Žilina, Slovakia)*
[2]*(Department of Electronic and Multimedia Communications, Faculty of Electrical Engineering and informatics/ University of Technology Košice, Košice, Slovakia)*
Corresponding Author:TomášIvaniga

Abstract: *This article focuses on the simulation of four-channel DWDM (Dense Wavelength Division Multiplexing) system with the spacing of 4 nm and the speed of 10 Gbps. It underlines the error rate BER (Bit Error Rate) which changes with the input power of fiber amplifier EDFA (Erbium Doped Fiber Amplifier) for the respective channel of DWDM. Nowadays while designing the DWDM it cannot be done without software tools simulating a real network to avoid possible mistakes which could occur before the actual construction of communication systems. Simulation solves the creation of DWDM from 1554 to 1566 nm with the best error rate for the respective channel using single-mode optical fiber 40 km long with measurable attenuation constant according to ITU-T G-652.D.*

Date of Submission: 14-01-2019 Date of acceptance: 29-01-2019

I. Introduction

Nowadays in terms of the working range financial costs of the wavelengths and generated profit the most suitable optical amplifier for DWDM systems is the EDFA amplifier formed by the doped ions Er^{3+}. These ions have the ability to absorb radiation in the spectrum around a wavelength of 1550 nm[1-3]. The amplifier requires pumping the wavelength of 980 nm to connect the input of a laser operating at this wavelength. The technology amplifiers for erbium base doped fiber are used for WDM systems. Their task is to amplify all the WDM channels at once and without the change of optical signal into electrical signal and back. The second chapter describes the EDFA principle and the connection for WDM systems [4]. The third chapter deals with the BER and Q - factor and their mutual dependency. The last chapter is the simulation representing the WDM with EDFA for the means of comparison of BER and Q-factor. The last chapter summarizes the results obtained from these simulations and describes the best error rate conforming to the channel with the given EDFA power.

II. The EDFA principle

Due to bound radiation from the pump laser (at a wavelength of 980 nm or 1480 nm) into the special fiber with a length of several meters (about 10 meters), a carbon doped element excitation happens - in this case erbium ions Er^{3+}. The absorbed energy enables the transition to a higher energy level E3 [5-8]. In this so-called metastable state the ions remain for a very short time (several milliseconds). This is followed by non-radioactive transition to the E2 levels in the conduction band. After reaching population inversion state, when the majority of erbium ions are in an excited state, due to the presence of the transmitted signal the energy is released.

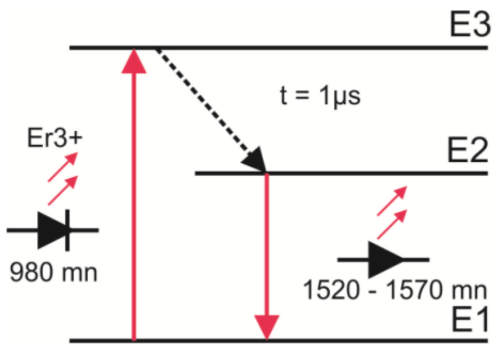

Fig. 1: The erbium excitation as a result of pumping radiation emission.

Following the return of the excited ions to the basic energy level E1 in the valence band accompanied by stimulated emission of radiation of the same wavelength and phase of the transmitted signal. This temporarily stores the energy obtained from the pump laser radiation. It amplifies transmitted optical signal at a wavelength of 1550 nm. During amplification the noise is amplified in the amplified band and spontaneous emission processes intensify (the natural transition of an electron to a lower level) [9], [10]. The amplification transmits optical signal at a wavelength of 1550 nm. Fig.1 illustrates the excitation of atoms due to erbium pumping radiation emission.

The EDFA connection

The optical amplifiers operate on the principle of stimulated emission of radiation for amplifying the input optical signal. The operating principle is very similar to the way lasers work. For generating new photons an amplifier has to be connected to the optical pump. This energy is either supplied by an electric field by a semiconductor amplifier or using pump radiation in the fiber amplifiers. With amplification a spontaneous emission noise can also occur (the natural transition of an electron to a lower level) called ASE (Amplified Spontaneous Emission) [11-13]. The EDFA is formed by a laser radiation source called a laser pump and a special optical fiber which is doped with erbium. Due to radiation from the laser pump the profit is generated in the telecom C band. The generated radiation is added to the signal in this band transmitting data [14], [15]. Fig. 2 shows a circuit diagram of the EDFA.For ensuring the optimal noise characteristics the EDFA amplifiers operate just below the saturation level. This reduces the spontaneous emission in the doped fiber and also noise and ASE.

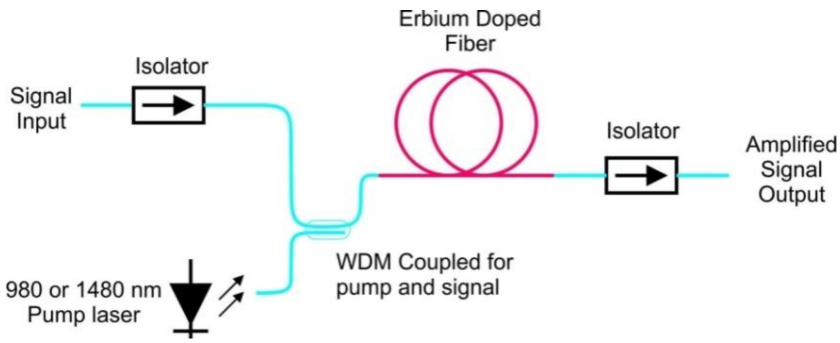

Fig. 2: The scheme of the EDFA connection.

III. BER and Q-Factor

BER is characteristic, very useful for finding out a system performance. BER parameter describes the ratio between bits wrongly detected and a total number of bits received (transmitted) [16-18]. As we can see in Fig. 3, there are two regions, *P (1/0)* and *P (0/1)*, needed to be discussed in detail.

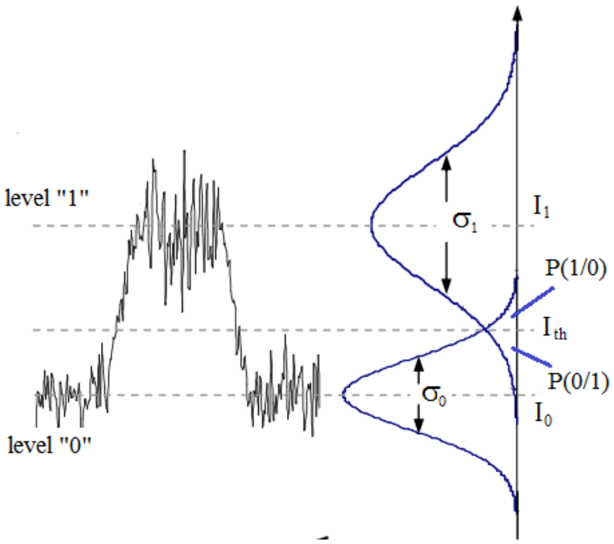

Fig. 3: Probability of a detection P(1/0) and P(0/1) with corresponding variances for level 1 and level 2 at the receiver end.

The information is detected in two levels, 0 and 1. These two levels have corresponded with current values I_0, I_1 as well as their variances σ_0, σ_1. The variances have usually different values. If the incoming signal has a value within σ_1, I_1region "*1*" is detected, the analogical process is applied with "*0*" level detection. However sometimes system makes an error and "*0*" is recognized when "*1*" was transmitted to *P(0/1),* as shown in Fig.3 (a lower region).Complementary "*1*" can be detected when "*0*" was sent to *P(1/0)* (a upper region) [15]. Corresponding probability functions are defined as follows:

$$P(0/1) = \frac{1}{\sqrt{2\pi}\sigma_1} \int_{-\infty}^{I_{th}} e^{-\frac{(I-I_1)^2}{2\sigma_1^2}} dI \quad , \tag{1}$$

$$P(1/0) = \frac{1}{\sqrt{2\pi}\sigma_0} \int_{I_{th}}^{\infty} e^{-\frac{(I-I_0)^2}{2\sigma_0^2}} dI \quad . \tag{2}$$

The next step is to define some complementary error functions for *P(0/1)* and *P(1/0)*:

$$P(0/1) = \frac{1}{2} erfc\left(\frac{I_1 - I_{th}}{\sigma_1\sqrt{2}}\right) , \tag{3}$$

$$P(1/0) = \frac{1}{2} erfc\left(\frac{I_{th} - I_0}{\sigma_0\sqrt{2}}\right) . \tag{4}$$

BER has the minimum value when *P(0/1)* and *P(1/0)* regions are equal [14], [17]. From this assumption we have to set the following condition for a threshold current I_{th} which is important to be set correctly:

$$\frac{I_1 - I_{th}}{\sigma_1} = \frac{I_{th} - I_0}{\sigma_0} \quad \Rightarrow \quad I_{th} = \frac{\sigma_0 I_1 + \sigma_1 I_0}{\sigma_1 + \sigma_0} . \tag{5}$$

Now we can define another parameter called Q – factor, shown in equation:

$$Q = \frac{I_1 - I_0}{\sigma_1 + \sigma_0} . \tag{6}$$

Q – factor describes the margin between two levels, "*0*" and "*1*", and their relation to the corresponding variances σ_1,σ_2. By assuming that BER is a sum of the regions shown in equations (3,4) we can define the following equation:

$$BER = \frac{1}{4}\left\{ erfc\left(\frac{I_1 - I_{th}}{\sigma_1\sqrt{2}}\right) + erfc\left(\frac{I_{th} - I_0}{\sigma_0\sqrt{2}}\right)\right\} . \tag{7}$$

Now it is possible to write a final equation for BER as well as its approximation by using exponential function as shown in the following equation:

$$BER = \frac{1}{2} erfc\left(\frac{Q}{\sqrt{2}}\right) \approx \frac{e^{-\frac{Q^2}{2}}}{Q\sqrt{2\pi}} . \tag{8}$$

IV. The simulation of DWDM system with different pumping EDFA

For simulating eye diagram and EDFA spontaneous emission was created a topology of a four-channel DWDM system (with a channel spacing of 4 nm) was generated.Fig. 4 shows the topology of a DWDM system.

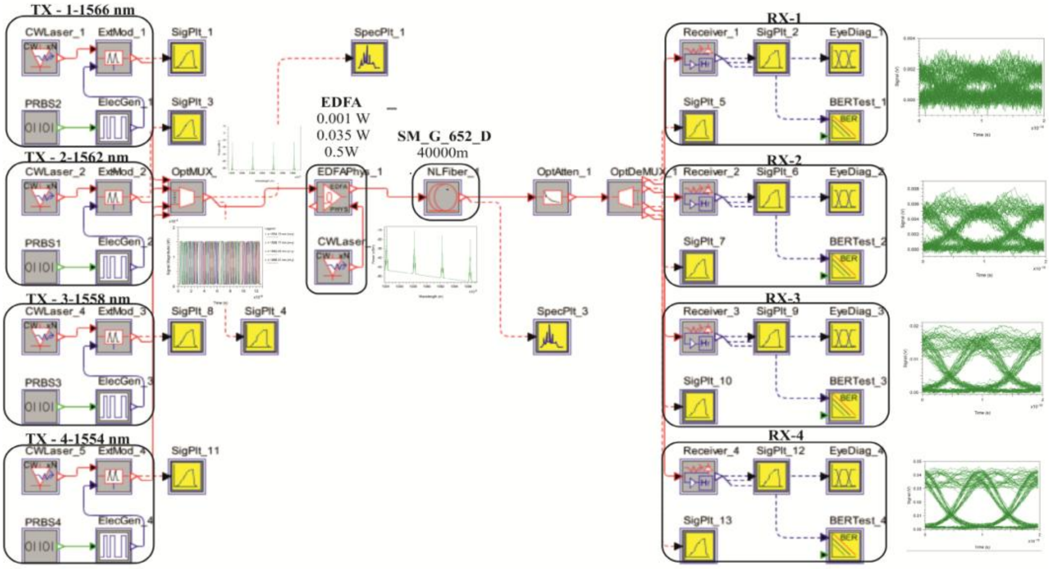

Fig. 4: The topology of a four-channel WDM system.

The whole topology consists of four transmitters (TX-1, TX-2, TX-3, TX-4) of the transmitting part and four receivers (RX-1, RX-2, RX-3, RX-4). Each TX includes: CW laser, an external modulator, an electric signal generator and data source (PRBS). PRBS has a set bit rate at 10 Gbps. CW lasers have set peak power at 0.01 W. The electric generator is used by the modulation format type Non Return to Zero (NRZ) with a filter type Ring Filter. The last component in the transmitter is an external modulator that uses modulation type MachZehnder. Fig. 5 shows the output of the transmitting part of the optical multiplexor.

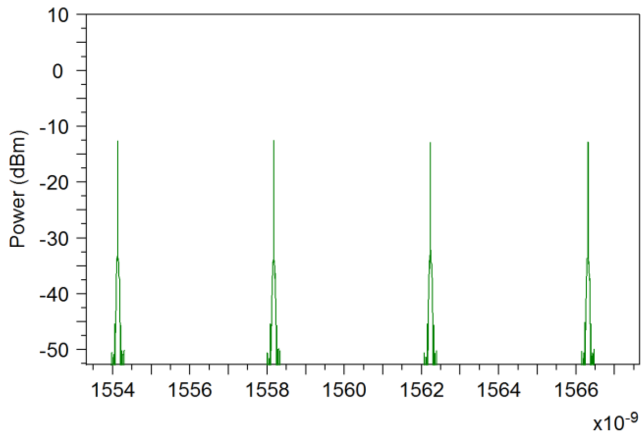

Fig. 5: The output of the transmitting part.

Behind the transmitting part is the transferring part consisting of: optical multiplexor, optical demultiplexor, EDFA, optical fiber, CW laser and a component for the attenuation of the transmitted route. All signals enter the optical multiplexor which uses the Trapezoidal filter and is set to 3dB. Table 1 offers values of the four receivers as the output for the optical multiplexor.

Table 1: Values of four transmitters

	TX1	TX2	TX3	TX4
Wavelength[nm]	1566	1562	1558	1554
Frequency[THz]	191399	191899	192399	192900
Average [dBm]	-11.204	-11.200	-11.004	-11.078
Pattern length	128			
Time step [s]	$3.125 \cdot 10^{-12}$			
Bitrate [bps]	10000000000			

The overall output of the optical multiplexor is -5.0998 dBm. During simulations we used single-mode optic fiber according to the standard in ITU-T G-652-D, length of 40 000 m with measurable attenuation constant of 0.3 dB/km. Optical attenuation of the transmission part was set to constant -5 dB. We also used optical amplifier EDFA with 3 pump powers by CW laser with the powers of: 0.01 W, 0.035 W and 0.5 W. In Fig.6 the influence of the spontaneous emission can be observed within the testing regime of EDFA.

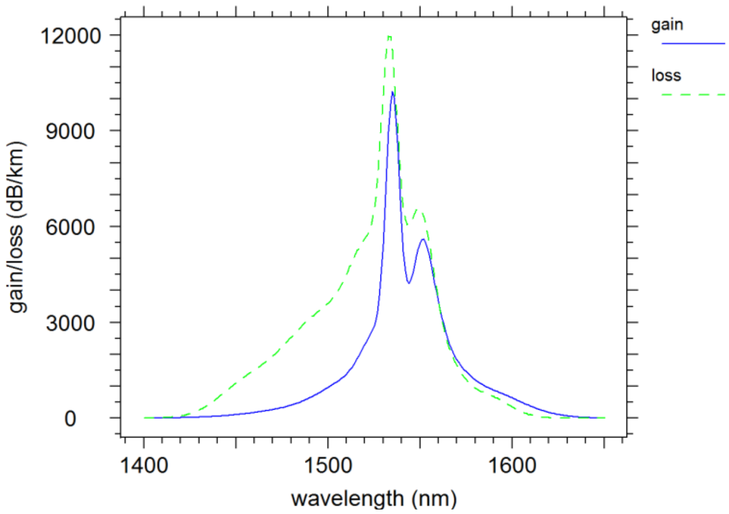

Fig. 6: The influence of the spontaneous emission EDFA.

In Fig. 7 we can see the optical spectrum of the EDFA amplification at a wavelength of 980 nm with a three different pumping powers: 0.01 W, 0.035 W and 0.5 W.

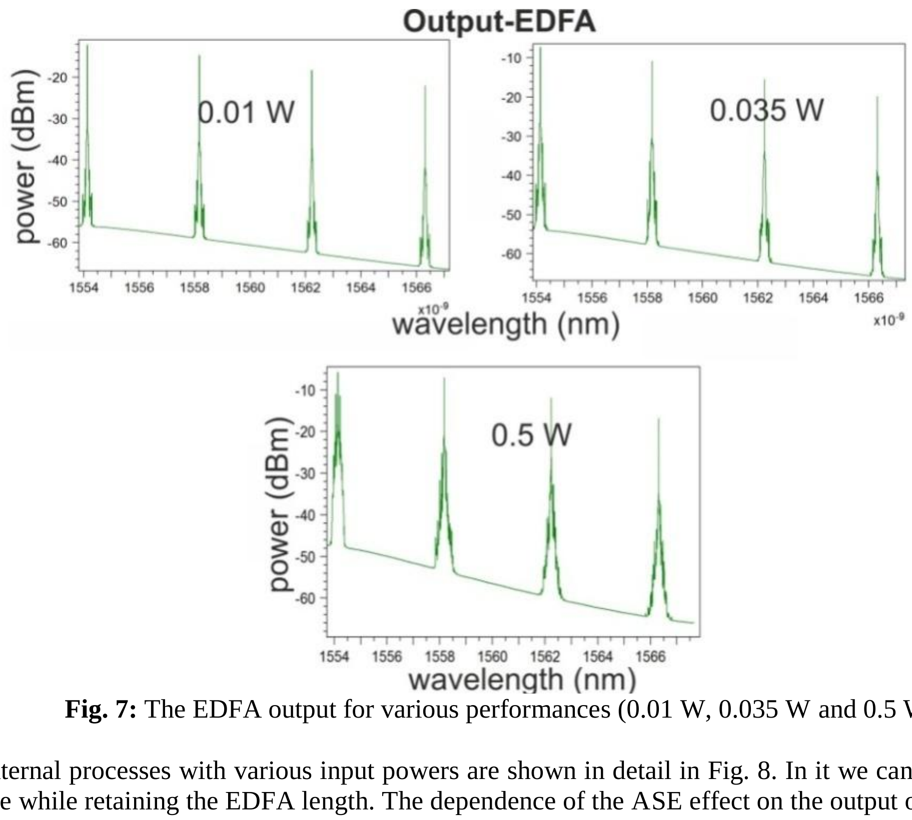

Fig. 7: The EDFA output for various performances (0.01 W, 0.035 W and 0.5 W).

The EDFA internal processes with various input powers are shown in detail in Fig. 8. In it we can see the input signal increase while retaining the EDFA length. The dependence of the ASE effect on the output of CW laser is shown in Fig. 8.

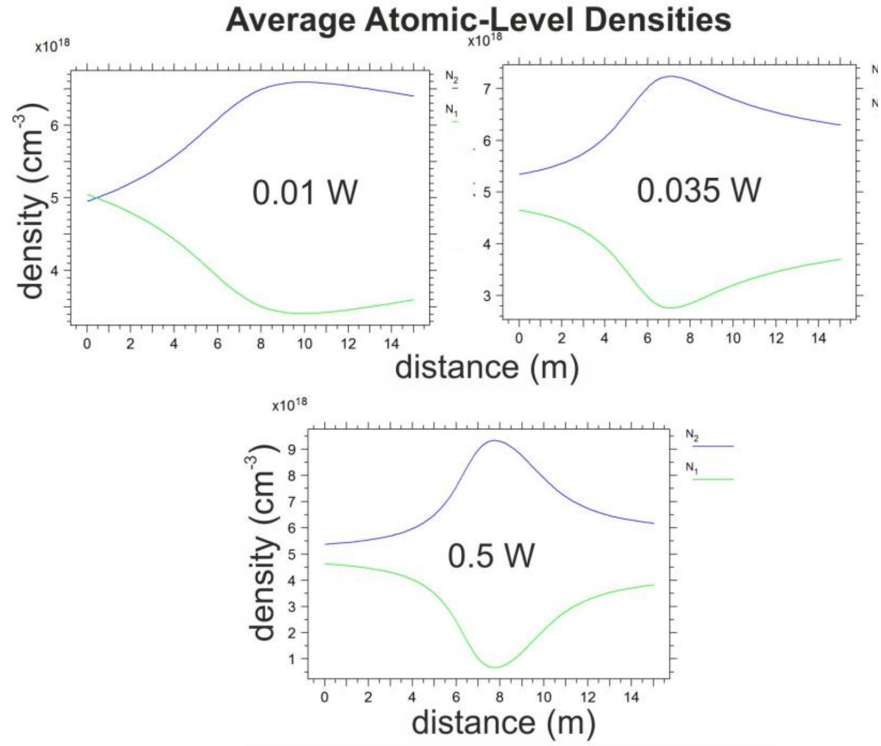

Fig. 8: The density state of erbium with various powers (0.01 W, 0.035 W and 0.5W) and constant length.

The ASE noise is approximately eliminated in proportion to the increasing input signal. The higher value (input) activates (excites) more erbium to a significant amplification. The smaller part of the erbium is therefore used to amplify spontaneous emission and can be seen in Fig. 9.

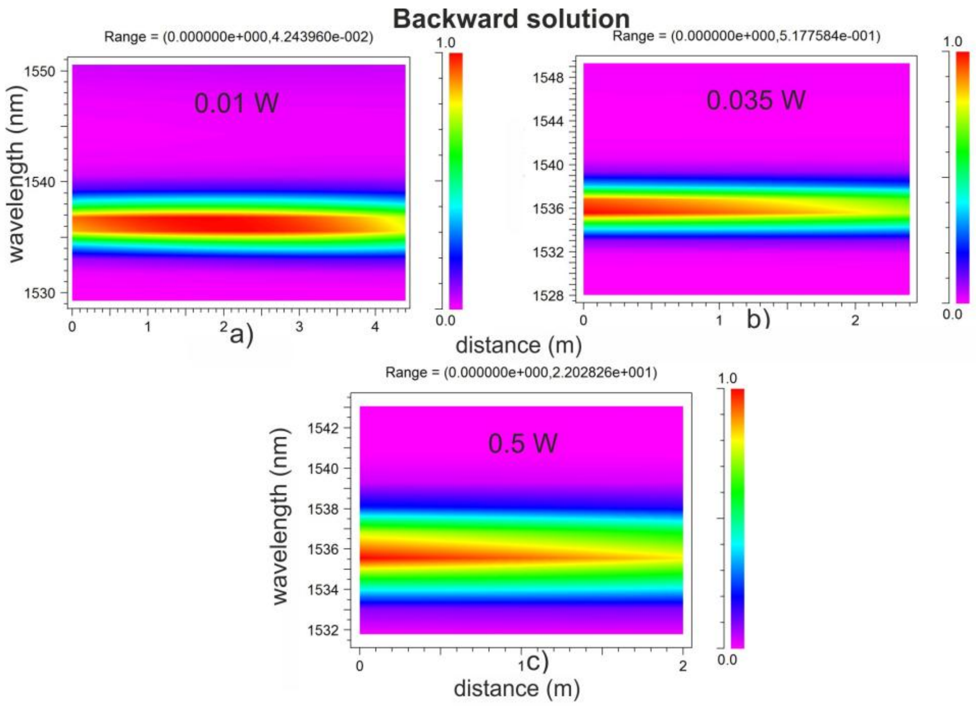

Fig. 9: The ASE spread with various input powers (0.01 W, 0.035 W and 0.5 W).

At the end of the transmission part is the optical demultiplexor which uses Trapezoidal filter with attenuation of 3 dB. In Table 2 are the output values of the amplifier entering the optical demultiplexor.

Table 2: The output values of the amplifier

	TX1	TX2	TX3	TX4
Wavelength[nm]	1.566	1.562	1.558	1.554
Frequency[THz]	191399	191899	192399	192900
Average [dBm] **0.01W** **0.035W** **0.5W**	-25.33 -23.11 -19.72	-21.641 -18.660 -14.403	-18.091 -13.966 -8.3520	-15.532 -10.180 -3.0284
Peak noise density[dBm/Hz] **0.01W** **0.035W** **0.5W**	-127.55477769521026 -119.99091182624034 -106.54101404945537			
Total average power [dBm] **0.01W** **0.035W** **0.5W**	-12.735420576736415 -8.1133573717968908 -1.6059468267977888			
Pattern length [bits]	128			
Time step [s]	$3.125 \cdot 10^{-12}$			
Bitrate [bps]	10000000000			

The receiving part consists of a PIN photodiode, preamplifier and Bessel filter connected to one component. Fig. 10 shows the eye diagrams for the receiver #1 with EDFA input powers: 0.01 W, 0.035 W and 0.5 W. In Table 3 are the output values for the receiver #1.

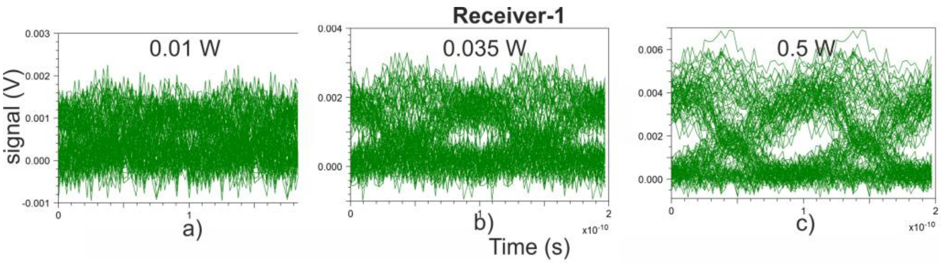

Fig. 10: The eye diagrams for the receiver #1 with powers (0.01 W, 0.035 W and 0.5 W).

Table 3: Final values for the receiver #1

Receiver #1 [W]	0.01	0.035	0.5
Average [V]	0.000523	0.000869	0.001897
Average Power[V^2]	$4.81941 \cdot 10^{-7}$	$1.34955 \cdot 10^{-6}$	$6.38660 \cdot 10^{-6}$
Avg. noise std. dev. [V]	0.000332	0.000333	0.000335
BER	$7.8143 \cdot 10^{-1}$	$1.5864 \cdot 10^{-2}$	$1.8121 \cdot 10^{-3}$
Q	1.4177	2.1478	3.5660

Fig.11 indicates the eye diagrams for the receiver #2 with input powers EDFA: 0.01 W, 0.035 W and 0.5 W. In Table 4 are the final values for the receiver #2.

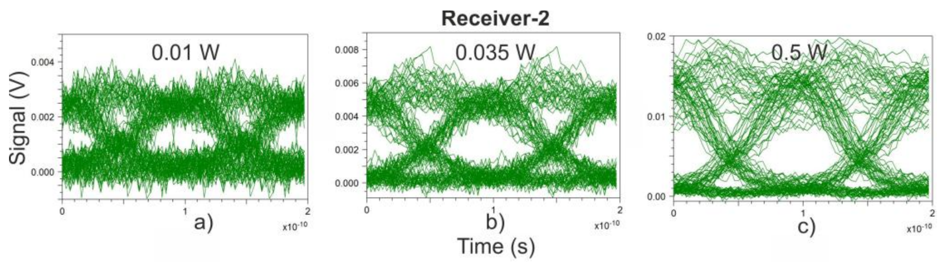

Fig. 11: The eye diagrams for the receiver #2 with powers (0.01 W, 0.035 W and 0.5 W).

Table 4: Final values for the receiver #2

Receiver #2 [W]	0.01	0.035	0.5
Average [V]	0.001225	0.002433	0.006486
Average Power [V^2]	$2.65080 \cdot 10^{-6}$	$1.04983 \cdot 10^{-5}$	$7.71763 \cdot 10^{-5}$
Avg. noise std. dev. [V]	0.000334	0.000337	0.000352
BER	$7.2143 \cdot 10^{-3}$	$4.3103 \cdot 10^{-6}$	$3.6651 \cdot 10^{-12}$
Q	3.1859	4.9208	9.1227

In Fig. 12 are shown the eye diagrams for the receiver #3 with EDFA input powers: 0.01 W, 0.035 W and 0.5 W. In Table 5 are the final values for the receiver #3.

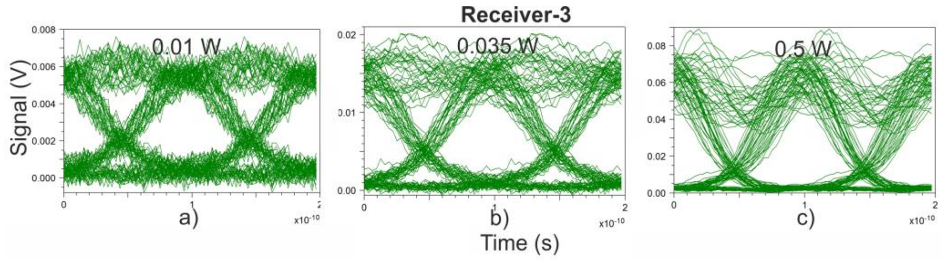

Fig. 12: The eye diagrams for the receiver #3 with powers (0.01 W, 0.035 W and 0.5 W).

Table 5: Final values for the receiver #3

Receiver #3 [W]	0.01	0.035	0.5
Average [V]	0.002767	0.007155	0.026062
Average Power [V^2]	$0.00276 \cdot 10^{-5}$	$9.08898 \cdot 10^{-5}$	$0.00134 \cdot 10^{-5}$
Avg. noise std. dev. [V]	0.000341	0.000360	0.000499
BER	$1.4285 \cdot 10^{-8}$	$6.9670 \cdot 10^{-15}$	0.0000
Q	6.3063	12.265	---

Fig. 13 shows the eye diagrams for the receiver #4 with EDFA input powers: 0.01W, 0.035W and 0.5W. In Table 6 are the final values for the receiver #4.

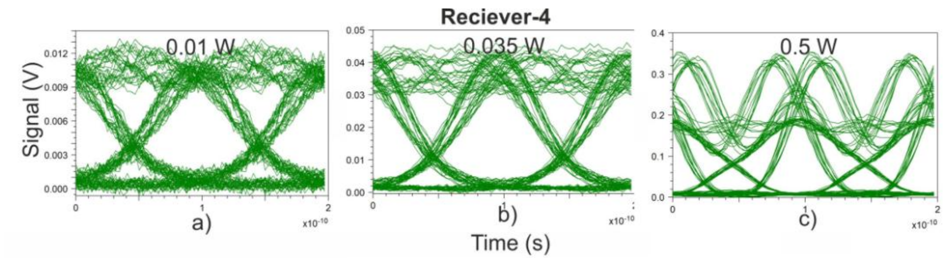

Fig. 13: The eye diagrams for the receiver #4 with powers (0.01 W, 0.035 W and 0.5 W).

Table 6: Final values for the receiver #4

Receiver #4[W]	0.01	0.035	0.5
Average [V]	0.004976	0.017048	0.088577
Average Power [V^2]	$4.33408 \cdot 10^{-5}$	0.000535267	0.017331027
Avg. noise std. dev. [V]	0.000357	0.000440	0.001175
BER	$3.2806 \cdot 10^{-16}$	$4.0797 \cdot 10^{-18}$	0.0000
Q	13.951	14.929	---

V. Conclusion

This article offered the simulation of the four-channel DWDM system with the wavelengths of 1566nm, 1562nm, 1558 nm and 1554nm with three pump powers of EDFA (0.01 W,0.35 W and 0.5 W) with the transmitting speed of 10Gbps. On the input side there were the quantitative parameters of Q and BER evaluated for the respective receivers. With the eye diagrams showed in Fig. #10-13 it is clear that the best results of the eye diagram and error rate parameters are listed in Table 6 for the receiver #4 which operates on the wavelength of 1554 nm. In keeping with the theoretical proposition the error rate and the Q-factor worsen as the wavelength increases.

References

[1]. G.Deshmukh, S. Jagtap , "*Four Wave Mixing in DWDM Optical System*", International Journal of Computational Engineering Research, vol. 3, no. 6, 2013, pp.07-11.

[2]. T. Huszaník, Ľ. Ovseník, J. Turán, *"Performance AnalysisofOpticalModulationFormatsfor 10 Gbit/s DWDM System"*, CarpathianJournalofElectronic and ComputerEngineering, vol. 10, no. 2, 2017, pp. 3-8.

[3]. Ľ. Mikuš, *"Evaluations of the error rate in backbone networks"*, Elektrorevue, vol. 12, no. 2, 2010, pp. 1-6.

[4]. T. Ivaniga, P. Ivaniga, *"Thedevelopmentof DWDM using OADM to influence a non-lineareffect SBS"*, ARPN JournalofEngineering and AppliedSciences, vol. 13, no. 13, 2018, pp. 4185-4194.

[5]. I. Rasheed, M. Abdullah, S. Mehmood, M. Chaudhary , *"Analyzing the non-linear effects at various power levels and channel counts on the performance of DWDM based optical fiber communication system"*, Emerging Technologies (ICET), 2012 International Conference, 2012, pp. 1-9, doi: 10.1109/ICET.2012.6375446.

[6]. ITU-T, G.694.1 (2012) Spectral Grids for WDM Applications: DWDM Frequency grid.

[7]. ITU-T, G.694.2 (2013) Spectral Grids for WDM Applications: CWDM Frequency grid.

[8]. O. Arora, A. K. Garg, S. Punia, *”Symmetrical Dispersion Compensation For High Speed Optical Links”*, IJCSI International Journal of Computer Science Issues, vol. 8 ,no. 1, 2011, pp. 371-376.
[9]. S. Kumar, M. J. Deen, *”Fiber Optic Communications: Fundamentals and Applications”,* Wiley-IEEE Press, ISBN: 978-0-470-51867-0, 2014, 572 pp.
[10]. M. Bhutani, A. Gagneja, *”Optical Transmission System Simulation for Analysis of Self Phase Modulation Non Linearity”*, International Journal of Scientific & Engineering Research, vol. 4, no. 6, 2013, pp. 1707-1713.
[11]. T. Ivaniga, P. Ivaniga, “*Comparison of the optical amplifiers EDFA and SOA based on the BER and Q-factor in C-band*”, Advances in Optical Technologies, 2017, pp.1-9. doi:10.1155/2017/9053582.
[12]. J. Smiesko, *“Exponential model oftokenbucketsystem“*, Komunikacie, vol. 5, no.4, pp.66-70.
[13]. P. Liptai, M. Moravec, E Lumnitzer, K. Lukačová, *”Impact analysis of the electromagnetic fields of transformer stations close to residential buildings”*. In: SGEM 2014, vol. 1, 2014, pp. 355-360.
[14]. P. Ivaniga, T. Ivaniga, *“Comparison of DPSK and RZ-DPSK Modulations in Optical Channel with Speed of 10 Gbps“*, Journal of Information and Organizational Sciences, vol. 41, no. 2, 2017, pp. 185-196, doi.org/10.31341/jios.41.2.4.
[15]. P. Liptai, M. Moravec, M. Badida, *”Research of possibilities of using the recycled materials based on rubber and textiles combined with vermiculite material in the area of noise reduction”*, Advanced Materials Research, vol. 1001, 2014, pp. 171-176.
[16]. Ľ. Mikuš, *”LMS systém Moodle”*, E-learn Žilina 2004, ISBN 80-8070-190-3, 2004, pp. 243-248.
[17]. D. Sharma, S. Kumar,*”Network blocking probability-basedevaluationofproposedspectrumassignmentstrategyfor a designedelasticoptical network link”,* Journal of Optics, vol. 47, no. 4, 2018, pp. 496-503.
[18]. T. Ivaniga, P. Ivaniga, Ľ. Ovseník, J. Turán, *“Nonlinear Effects in Fully Optical Communications Systems”*, ISBN: 978-80-7365-412-2, 2019, 209 pp.

IOSR Journal of Electronics and Communication Engineering (IOSR-JECE) is UGC approved Journal with Sl. No. 5016, Journal no. 49082.

Petr Ivaniga. "The Influence of Bit Error Rate on DWDM System with Different Pumping Powers in EDFA." IOSR Journal of Electronics and Communication Engineering (IOSR-JECE) 14.1 (2019): 22-30.